J. Fluid Mech. (1984), *vol.* 139, *pp.* 219–235
Printed in Great Britain

Long waves induced by short-wave groups over an uneven bottom

By CHIANG C. MEI AND CHAKIB BENMOUSSA
Parsons Laboratory, Department of Civil Engineering, Massachusetts Institute of Technology

(Received 16 February 1983 and in revised form 20 September 1983)

Unidirectional and periodically modulated short waves on a horizontal or very nearly horizontal bottom are known to be accompanied by long waves which propagate together with the envelope of the short waves at their group velocity. However, for variable depth with a horizontal lengthscale which is not too great compared with the group length, long waves of another kind are further induced. If the variation of depth is only one-dimensional and localized in a finite region, then the additional long waves can radiate away from this region, in directions which differ from those of the short waves and their envelopes. There are also critical depths which define caustics for these new long waves but not for the short waves. Thus, while obliquely incident short waves can pass over a topography, these second-order long waves may be trapped on a ridge or away from a canyon.

1. Introduction

Moored vessels, tension-leg platforms and some small harbours have natural periods on the order of a few minutes; therefore they are not resonated directly by wind waves whose typical periods are around 10 s. However, the incident sea is seldom uniform, and the modulational periods of short waves can be in the range of a few minutes. It is known from the theory of radiation stresses (Longuet-Higgins & Stewart 1960, 1961, 1962) that long waves collinear with respect to, and of the same period as, the short-wave envelope can be induced by nonlinearity and then propagate with the envelope, provided that the lengthscale of depth variation is much greater than the group length. It is further known for a semi-infinite tank of uniform cross-section that paddle-generated wave groups can radiate these two kinds of long waves (Hansen 1978; Sand 1981). The radiation stress theory has also been used by Longuet-Higgins & Stewart (1962) to infer qualitatively that waves breaking on a beach can induce seaward long waves which propagate at the speed $(gh)^{\frac{1}{2}}$. At the other extreme, a steady train of obliquely incident waves breaking on a beach can induce steady longshore currents (Bowen 1969; Thornton 1970; Longuet-Higgins 1970*a*, *b*). Here the group length is infinite compared with the topographical lengthscale, so that the long waves become the current in the limit. Recent interest has been on the third case where the two lengthscales are comparable. For example, Bowers (1977) studied a one-dimensional channel of constant depth but discontinuous width, the length of one width being finite and the other infinite. Modulated wave groups incident from infinity are found to induce long waves propagating at the speed $(gh)^{\frac{1}{2}}$ and excite resonance in the section of finite length. More recently, Molin (1982) has considered short-wave groups in fairly deep water ($kh \gg 1$) *normally* incident on a one-dimensional topography, while the group length is nevertheless much greater than the water depth. Long waves of speed $(gh)^{\frac{1}{2}}$ are found to radiate away in both directions from the zone of variable depth. Because of the large-kh assumption the amplitude of the radiated long waves is much weaker than A^2k, where A is the typical amplitude of the short waves. Although some numerical results have also been presented by Molin for $kh = O(1)$, they appear to have been based on an incomplete theory.

In this paper, we extend Molin (1982) and study long waves caused by short-wave groups over slowing varying depth. We assume that the lengthscales of wave modulation and of depth change are comparable. The depth is intermediate relative to the short wavelength, $kh = O(1)$, and varies so slowly that reflection of short waves is unimportant yet not so slowly that the forced long waves are no less than $O(kA^2)$.† In §2 the governing equations based on geometric-optics approximation for waves over two-dimensional topography $h = h(x, y)$ are given. The remaining parts of the paper are limited to one-dimensional topography $h = h(x)$, with emphasis on oblique incidence. In §3 the variation of the short wave and the steady set-down are examined. In §4 we discuss the long wave locked to the short-wave envelope and the free long wave radiated away from the zone of variable depth. The amplitudes of these radiated waves are found in §5 by looking into the zone of variable depth. The influence of the short-wave incidence angle is discussed for shelves, ridges and canyons of different width. Waveguide effects are pointed out.

2. General governing equations

Consider a train of slowly modulated sinusoidal waves over a slowly varying two-dimensional topography. We assume that the length- and timescales of the groups are $O(\epsilon^{-1})$ times those of the incident short waves, where $\epsilon \ll 1$. Specifically the wavenumber and frequency of the envelope are ϵk_0 and $\epsilon\omega C_{g_0}/C_0$ respectively, where k_0 and ω are the wavenumber and frequency, and C_{g0} and C_0 the group and phase velocities of the short waves over the constant reference depth h_0. We further assume that the slopes of both the short waves and the depth h are $O(\epsilon)$. Introducing the slow variables

$$\left.\begin{aligned} \bar{\boldsymbol{x}} &= \epsilon \boldsymbol{x}, \quad \text{with} \quad \boldsymbol{x} = (x, y), \\ \bar{t} &= \epsilon t, \end{aligned}\right\} \tag{2.1}$$

we have the first-order velocity potential and free-surface displacement

$$\phi = -\frac{\mathrm{i}gA}{2\omega}\frac{\operatorname{ch} k(z+h)}{\operatorname{ch} kh}\exp \mathrm{i}\left(\int \boldsymbol{k}(\boldsymbol{x})\cdot \mathrm{d}\boldsymbol{x} - \omega t\right) + *, \tag{2.2}$$

$$\zeta = \tfrac{1}{2}A \exp \mathrm{i}\left(\int \boldsymbol{k}(\bar{\boldsymbol{x}})\cdot \mathrm{d}\boldsymbol{x} - \omega t\right) + *. \tag{2.3}$$

Here $*$ denotes the complex conjugate of the preceding term, $A(\bar{\boldsymbol{x}}, \bar{t})$ is the amplitude, $h(\bar{\boldsymbol{x}})$ the still-water depth and $\boldsymbol{k}(\bar{\boldsymbol{x}})$ the local wavenumber governed by the dispersion relation

$$\omega^2 = gk \operatorname{th} kh \quad \text{with} \quad k = |\boldsymbol{k}|. \tag{2.4}$$

The frequency ω of the short wave is taken to be constant; slow variations in time are contained in the amplitude $A(\bar{x}, \bar{t})$. It is well known that

$$\frac{\partial k_x}{\partial \bar{y}} - \frac{\partial k_y}{\partial \bar{x}} = 0, \tag{2.5}$$

† Typical numerical values are as follows: short-wave period = $O(10$ s), depth $O(20$ m), group and long-wave period $O(100$ s), group and topography length $O(100$ m), short-wave amplitude $O(3$ m) and long-wave amplitude $O(0.3$ m).

and
$$\frac{\partial |A|^2}{\partial \bar{t}} + \bar{\nabla}\cdot(C_g|A|^2) = 0, \quad \text{with} \quad \bar{\nabla} = \left(\frac{\partial}{\partial \bar{x}}, \frac{\partial}{\partial \bar{y}}\right). \tag{2.6}$$

Note that on constant depth A must be a function of $\boldsymbol{k}\cdot\bar{\boldsymbol{x}}/k - C_g\bar{t}$. At the second order the mean sea level $\xi(\bar{\boldsymbol{x}},\bar{t})$ and the induced long-wave velocity $\boldsymbol{U}(\bar{\boldsymbol{x}},\bar{t})$ satisfy the equations

$$\frac{\partial \xi}{\partial \bar{t}} + \bar{\nabla}\cdot\left(h\boldsymbol{U} + \frac{\boldsymbol{k}}{\omega}\frac{g|A|^2}{2}\right) = 0, \tag{2.7}$$

$$\frac{\partial \boldsymbol{U}}{\partial \bar{t}} + g\bar{\nabla}\xi + \frac{\omega^2}{2g}\bar{\nabla}\left(\frac{g|A|^2}{2\,\mathrm{sh}^2\, kh}\right) = 0, \tag{2.8}$$

which were deduced in this form by a WKB procedure under the present assumptions of scales (Chu & Mei 1970). We stress that these equations hold only in the range $\bar{\boldsymbol{x}}, \bar{t} = O(1)$; for larger spatial and time domains wave instability is important and higher-order effects must be considered. Also, since ϵ does not appear explicitly, our results are independent of ϵ as long as it is sufficiently small. If $\boldsymbol{U}$ is eliminated by cross-differentiation, then

$$\bar{\nabla}\cdot gh\,\bar{\nabla}\xi - \frac{\partial^2 \xi}{\partial \bar{t}^2} = \frac{\partial}{\partial \bar{t}}\bar{\nabla}\cdot\left(\frac{\boldsymbol{k}g|A|^2}{2\omega}\right) - \bar{\nabla}\cdot h\bar{\nabla}\left(\frac{\omega^2|A|^2}{4\,\mathrm{sh}^2\, kh}\right). \tag{2.9}$$

Since the radiation stress tensor for the progressive wave (2.2) is

$$\boldsymbol{S} = \frac{\rho g A^2}{2}\left[\left(\frac{C_g}{C} - \frac{1}{2}\right)\boldsymbol{I} + \frac{C_g}{C}\boldsymbol{kk}\right][1 + O(\epsilon^2)], \tag{2.10}$$

we may re-express, after some algebra, (2.9) as

$$\bar{\nabla}\cdot gh\bar{\nabla}\xi - \frac{\partial^2 \xi}{\partial t^2} = \frac{1}{\rho}\bar{\nabla}\cdot(\bar{\nabla}\cdot\boldsymbol{S}) + O(\epsilon^5). \tag{2.11}$$

In the limit of constant depth, (2.11) was derived and used for calculating the set-down and set-up of unidirectional wave groups by Longuet-Higgins & Stewart (1960, 1961, 1962). A similar equation with constant h also governs the sound wave generated by turbulence (see Lighthill 1952), in which case ξ corresponds to sound pressure and $\boldsymbol{S}$ the momentum flux tensor due to random fluctuations.

Our goal here is to study the long wave generated by variations in the radiation stress in an inhomogeneous medium.

The following normalization will be employed:

$$\left.\begin{aligned} &\bar{\boldsymbol{x}} \to \frac{\boldsymbol{X}}{k_\infty}, \quad \bar{t} \to \frac{T}{\omega}, \quad h \to \frac{h}{k_\infty}, \quad h_0 \to \frac{h_0}{k_\infty}, \quad k \to k_\infty k, \\ &A \to a_0 A, \quad \xi \to k_\infty a_0^2 \xi, \quad C_g \to \frac{\omega}{k_\infty} C_g, \end{aligned}\right\} \tag{2.12}$$

where the subscript zero refers to the constant depth h_0 and $k_\infty = \omega^2/g$. In terms of these normalized variables, the new forms of (2.5)–(2.11) are obtained simply by letting ω and g be unity, and will be omitted.

3. Short waves and steady set-down on the one-dimensional topography

For a general two-dimensional topography, the wave-action equation (2.6) must be solved numerically. Here we only focus our attention to the simpler case of straight and parallel contours $h = h(X)$. In this case

$$k = k(X), \quad k_x = k_x(X), \quad k_y = \text{constant}. \tag{3.1}$$

The local angle of incidence $\alpha(X)$ is defined by

$$k_x = k\cos\alpha, \quad k_y = k\sin\alpha = k_0 \sin\alpha_0. \tag{3.2}$$

Over constant depth, the simplest model for a slowly modulated wavetrain is the superposition of two colinear sinusoidal wavetrains of slightly different wavenumbers $\boldsymbol{k}_0 + \epsilon\boldsymbol{k}_0$ and $\boldsymbol{k}_0 - \epsilon\boldsymbol{k}_0$, with normalized amplitudes 1 and b, respectively, b being positive and real. The corresponding wave envelope is given by

$$A(X, Y, T) = \tfrac{1}{2}\exp[\mathrm{i}(k_{x0} X + k_{y0} Y - \Omega_0 T)] + \tfrac{1}{2}b\exp[-\mathrm{i}(k_{x0} X + k_{y0} Y - \Omega_0 T)], \tag{3.3}$$

where

$$\Omega = C_{g0} k_0. \tag{3.4}$$

We shall assume that the incident wave from the region $X < X_0$ where $h = h_0$ has this envelope. In the region of variable h the envelope is expected to be of the following form:

$$A(x, y, T) = \tfrac{1}{2}\tilde{A}(X)\exp\left[\mathrm{i}\left(\int_{X_0}^{X} K_x\,\mathrm{d}X + k_y\, Y - \Omega T\right)\right]$$
$$+ \tfrac{1}{2}b\tilde{A}(X)\exp\left[\mathrm{i}\left(\int_{X_0}^{X} K_x\,\mathrm{d}K + k_y\, Y - \Omega T\right)\right], \tag{3.5}$$

where $\tilde{A}(X)$ and $K_x(X)$ are real functions of X and $k_y = k_{y0} =$ constant. Substituting this into the dimensionless form of (2.6), we get from the real and imaginary parts respectively

$$\tilde{A}(X) = \left[\frac{(C_{gx})_0}{C_{gx}}\right]^{\frac{1}{2}}, \tag{3.6}$$

and

$$\Omega = K_x C_{gx} + k_y C_{gy}. \tag{3.7}$$

Dividing (3.7) by $\Omega = C_{g0} k_0$ we get

$$1 = \frac{C_g}{C_{g0}}\left(\frac{K_x k_x}{k_0 k} + \frac{K_y k_y}{k_0 k}\right); \tag{3.8}$$

hence the x-component of the envelope wavenumber vector can be written as

$$K_x = \frac{C_{g0} k_0}{C_{gx}} - \frac{k_y^2}{k_x} = k_x + \frac{k^2}{k_x}\left(\frac{C}{C_g}\frac{C_0}{C_{g0}} - 1\right), \tag{3.9}$$

which reduces to k_{x0} when $h = h_0$. For a fixed ω and increasing h, the ratio

$$\frac{C}{C_g}\Big/\frac{C_0}{C_{g0}} = \left(1 + \frac{2k_0 h_0}{\operatorname{sh} 2k_0 h_0}\right)\Big/\left(1 + \frac{2kh}{\operatorname{sh} 2kh}\right), \tag{3.10}$$

increases monotonically, hence K_x becomes increasingly greater than k_x. Now let h increase with X. For sufficiently large angle of incidence a caustic may exist such that $k_x \downarrow 0$; then $K_x \uparrow \infty$. There the short-wave crests are perpendicular to the caustic contour while the envelope crests are normal to it. On the other hand if h decreases with X from X_0, K_x falls below k_x, but the difference diminishes as $h \downarrow 0$. Sample numerical results are shown in figure 1 for the case where the dimensionless $h_0 = 0.5$. For a greater h_0, the ratio (3.9) and $K_x - k_x$ are smaller; the qualitative features of K_x and k_x versus h are the same as in figure 1. The behaviour of the envelope near a caustic requires a different approximation which should account for reflection; we shall postpone cases involving these caustics for future study.

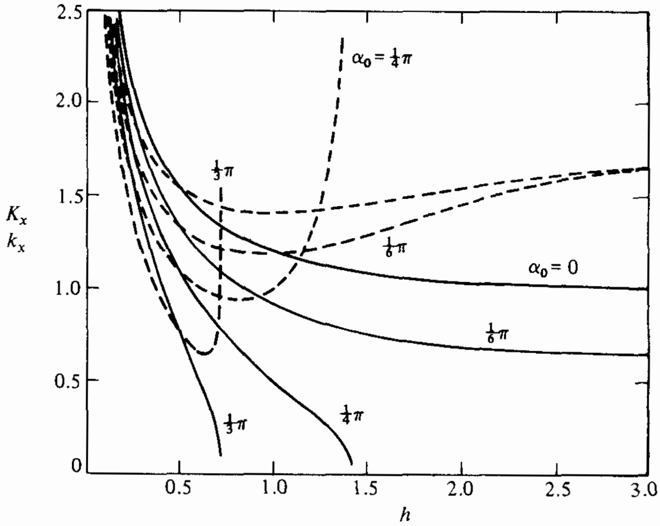

FIGURE 1. Dimensionless wavenumber components in the x-direction as functions of incidence angle α_0 and dimensionless local depth: ——, k_x for the short waves; ---, K_x for the envelope.

The wave envelope propagates in the direction β with respect to the X-axis where

$$\tan\beta = k_y/K_x, \tag{3.11}$$

while the dimensionless propagation speed of the envelope is

$$C_{\mathrm{E}} = \Omega(K_x^2+k_y^2)^{-\frac{1}{2}}. \tag{3.12}$$

If the depth changes from h_0 for $X < X_0$ to $h_1 \gtrless h_0$ for $X > X_1 > X_0$ then on the transmission side

$$K_{x1} \gtrless K_{x0} = k_{x0} \quad \text{so that} \quad \tan\beta_1 \lesseqgtr \tan\alpha.$$

In view of (2.9), we express the second-order mean sea level as

$$\xi = \xi_0(X)+\tfrac{1}{2}[\bar{\xi}(X)\exp 2\mathrm{i}(k_y\,Y-\Omega T)+*]. \tag{3.13}$$

The steady-state part corresponding to the zeroth harmonic of $|A|^2$ is

$$\xi_0 = -\frac{(1+b^2)\,(C_{gx})_0}{16C_{gx}\,\mathrm{sh}^2\,kh} = -\frac{(1+b^2)\,|\bar{A}|^2}{16\,\mathrm{sh}^2\,kh}, \tag{3.14}$$

which is the ordinary set-down of waves unmodulated in time. The amplitude $\bar{\xi}(X)$ is governed by the ordinary differential equation:

$$\frac{\mathrm{d}}{\mathrm{d}X}h\frac{\mathrm{d}\bar{\xi}}{\mathrm{d}X}+4(\Omega^2-k_y^2\,h)\,\bar{\xi} = \Bigg\{\left[\frac{kh(K_x^2+k_y^2)}{2\,\mathrm{sh}^2\,kh}+\frac{\Omega^2 k}{C_g}\right]\frac{b(C_{gx})_0}{C_{gx}}+\frac{2b}{1+b^2}\Bigg[\frac{\mathrm{d}}{\mathrm{d}X}h\frac{\mathrm{d}\xi_0}{\mathrm{d}X} +\mathrm{i}\left(4K_x\,h\frac{\mathrm{d}\xi_0}{\mathrm{d}X}+2\xi_0\frac{\mathrm{d}}{\mathrm{d}X}(K_x\,h)\right)\Bigg] -\frac{\mathrm{i}b}{2}\Omega(C_{gx})_0\frac{\mathrm{d}}{\mathrm{d}X}\left(\frac{k}{C_g}\right)\Bigg]\Bigg\}\exp\left(2\mathrm{i}\int_{X_0}^{X}K_x\,\mathrm{d}X\right), \tag{3.15}$$

where use has been made of (3.6).

We plot the steady set-down $\xi_0(X)$ in figure 2 for $b = 1$, $\alpha_0 = 0, \frac{1}{6}\pi, \frac{1}{4}\pi$, and $h_0 = 0.5$.

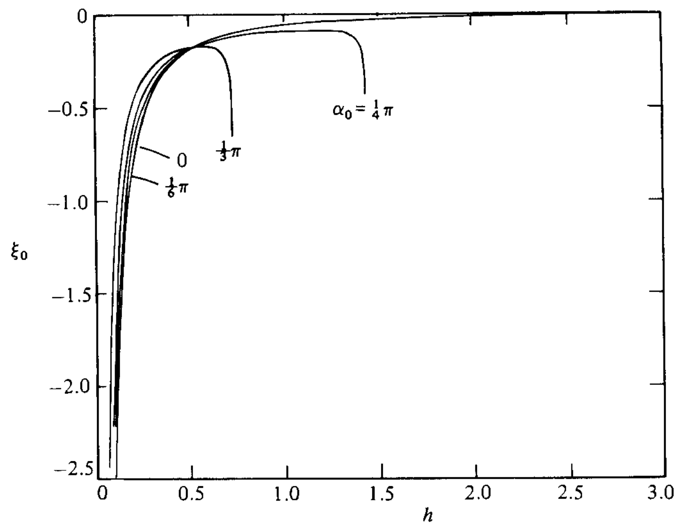

FIGURE 2. Steady-state set-down ξ_0 as a function of angle of incidence and local depth. Depth on incidence side $h_0 = 0.5$.

As $h \downarrow 0$, $\xi_0 \downarrow -\infty$; the weakly nonlinear theory is invalid here. For sufficiently large α_0, ξ_0 also becomes unacceptably large at the caustic; this can in principle be remedied by a locally refined theory.

4. Locked and free long waves on regions of constant depth

We now separate the amplitude $\xi(X)$ of the time-varying component into two parts: the *locked* waves and the *free* waves. Here we first examine the regions of constant depth.

For constant depth, the first [ ] on the right of (3.15) is constant and the remaining terms vanish; the particular solution is

$$\xi = \xi_L \exp\left(2\mathrm{i} \int_{X_0}^{X} K_x \,\mathrm{d}X\right), \tag{4.1}$$

with
$$\xi_L = -\frac{b}{8}\frac{(C_{gx})_0}{C_{gx}}\left(\frac{2kh(K_x^2+k_y^2)}{\mathrm{sh}^2\, kh} + \frac{2\Omega^2 k}{C_g}\right)\Big/[(K_x^2+k_y^2)\,h - \Omega^2]. \tag{4.2}$$

From (3.13) and (4.1), ξ_L travels in the same direction as the wave envelope (cf. (3.9)) but not in the direction of the short waves themselves. The waves described by ξ_L are called the *locked waves* as in Molin (1982). For $b = 1$ and normal incidence $\alpha_0 = \beta = 0$, ξ_L reduces to the well-known result of Longuet-Higgins & Stewart (1964):

$$\xi_L = -\frac{4kC_{g0} - 1}{8C_{g0}(h_0 - C_{g0}^2)}. \tag{4.3}$$

We plot ξ_L according to (4.2) in figure 3 for $b = 1$ and $h_0 = 0.5$; it qualitatively resembles ξ_0. The effect of angle of incidence is small. The large values near $h = 0$ and near the caustic are not reliable and correspond to the failure of the present theory.

From here on we assume the region of variable depth to be confined in $X_0 < X < X_1$ and let $h = h_0$ for $X < X_0$ and $h = h_1$ for $X > X_1$. In the zones of constant depth the complete solution for ξ is of the form

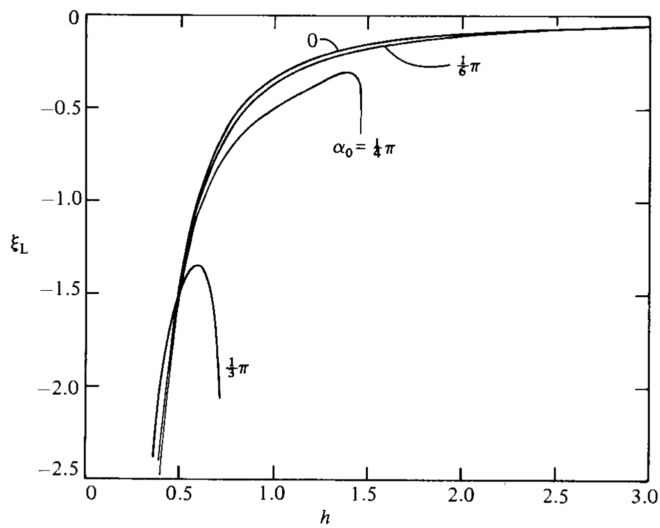

FIGURE 3. Amplitude ξ_L of locked long wave as a function of angle of incidence α_0 and local depth.

$$\left.\begin{aligned} \xi &= (\xi_L)_j \exp\left(2\mathrm{i}\int_{X_0}^{X} (K_x)_j \,\mathrm{d}X\right) + (\xi_F)_j \\ j &= \begin{pmatrix}0\\1\end{pmatrix} \quad \text{for} \quad X\begin{pmatrix}< X_0\\ > X_1\end{pmatrix}, \end{aligned}\right\} \tag{4.4}$$

with

where $(\xi_L)_{0,1}$ are given by (4.2). The remaining parts $(\xi_F)_{0,1}$ correspond to the *free waves*, which are the homogeneous solutions of (3.15) over depths h_0 and h_1. The behaviour of these unforced waves $(\xi_F)_{0,1}$ depends crucially on the sign of

$$\lambda_j^2 = \frac{1}{h_j}(\Omega^2 - k_y^2 h_j) = k^2\left(\frac{C_{g0}^2}{h_j} - \sin^2\alpha_0\right), \tag{4.5}$$

in these two regions. If $\lambda_j^2 > 0$, $(\xi_F)_j$ must be outgoing waves in the region $h = h_j$

$$\left.\begin{aligned} (\xi_F)_j &= B_j \exp(2\mathrm{i}|\lambda_j|\,|X|) \quad \text{if} \quad \lambda_j^2 > 0, \\ j &= \begin{pmatrix}0\\1\end{pmatrix} \quad \text{for} \quad X\begin{pmatrix}< X_0\\ > X_1\end{pmatrix}. \end{aligned}\right\} \tag{4.6}$$

These free waves propagate at the linear long-wave speed $C_j = h_j^{\frac{1}{2}}$ (or $(gh_j)^{\frac{1}{2}}$ in physical scale) and in the direction θ_j with

$$\tan\theta_j = (\operatorname{sgn} X)\, k_y/|\lambda_j|. \tag{4.7}$$

If $\lambda_j^2 < 0$, ξ_F attenuates exponentially:

$$\left.\begin{aligned} (\xi_F)_j &= B_j \exp(-2|\lambda_j|\,|X|), \\ j &= \begin{pmatrix}0\\1\end{pmatrix} \quad \text{for} \quad X\begin{pmatrix}< X_0\\ > X_1\end{pmatrix}. \end{aligned}\right\} \tag{4.8}$$

Thus these long waves can be trapped away from the region where $\lambda_j^2 < 0$. Trapping of long waves is of course well known in the linearized theory, as a consequence of

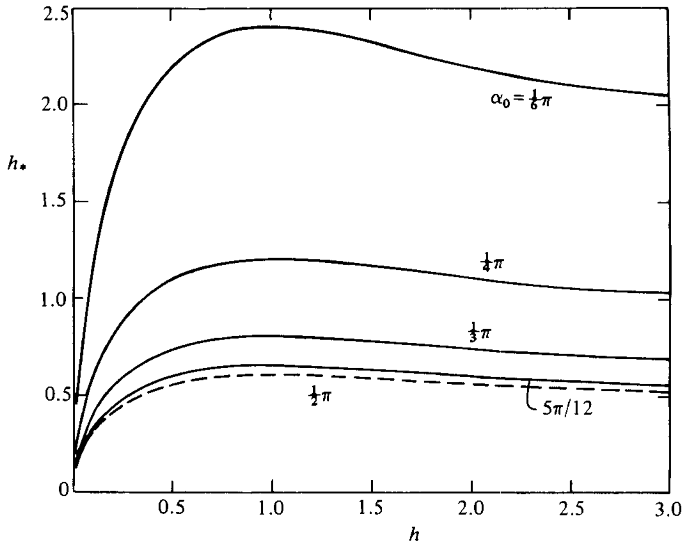

FIGURE 4. The critical depth h_* versus h_0 with α_0 as parameter. For $\alpha_0 = \frac{1}{2}\pi$ (dashed curve), $h_* = C_{g0}^2$.

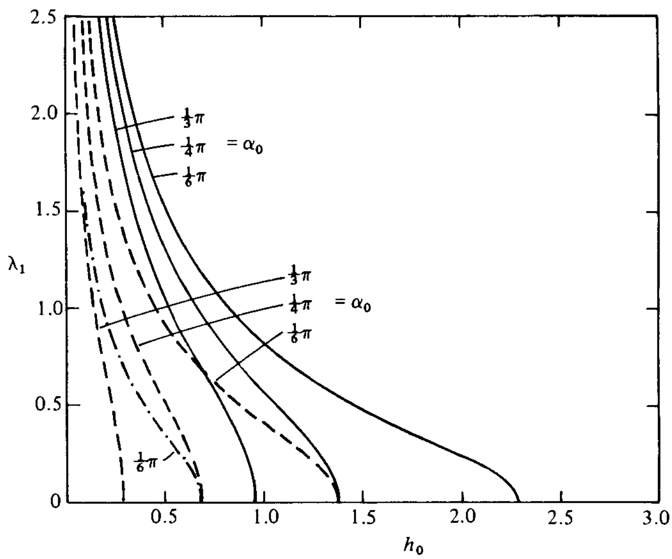

FIGURE 5. Dimensionless wavenumber component λ_1 in the x-direction of free long waves. The parameter is α_0. Solid curves: $h_0/h_1 = 2$. Dashed curves: $h_0/h_1 = 1$. Dot–dashed curve: $h_0/h_1 = 0.5$ and $\alpha_0 = \frac{1}{6}\pi$; λ_1 is imaginary for $\alpha_0 = \frac{1}{4}\pi$ and $\frac{1}{3}\pi$.

refraction (see e.g. Longuet-Higgins 1967); the added feature in the present problem is that the long-wave frequency is related to that of the short wave via (3.4). The critical depth $h = h_*$ at which $\lambda^2 = 0$ corresponds to the turning point of the differential equation (3.15). Consider the incidence side $h_j = h_0$. From (4.5), since $C_{g0}^2/h_0 = C_{g0}^2/C_0^2 < 1$, there always exists an h_* in $X_0 < X < X_1$ if α_0 is large enough so that

$$\sin \alpha_0 > C_{g0}/C_0.$$

If $h_1 = h_0$ then h_* may exist for two values of X, and long waves can be trapped between them. If h is monotonic in X in the region $X_0 < X < X_1$ there can be only one h_*.

The value of $h_* = C_{g0}^2/\sin^2\alpha_0$ depends on h_0 and α_0 as shown in figure 4. Clearly h_* is greater for smaller α_0. As is well known in the classical theory of normally incident shoaling waves (Burnside 1915), for increasing h_0, C_{g0} first increases to a maximum at $h_0 \approx 1$ or $k_0 h_0 \approx 1.2$, then decreases to the asymptotic limit $\frac{1}{2}$ ($= g/2\omega^2$ in physical terms, see the dashed curve in figure 4). Correspondingly, h_* first increases to a maximum then to the asymptotic limit $(2\sin\alpha_0)^{-2}$. To have some idea of the direction of the radiated free waves, we plot in figure 5 λ_1 (real) as a function of h_0 with h_0/h_1 and α_0 as parameters. Note that the curves for $h_0/h_1 = 1$ also give $\lambda_0 = \lambda_1$, and hence the direction of free waves on both sides of the depth transition. The monotonic decline of λ_1 with increasing h_0 is caused by similar behaviour of k_0. In particular, $k_0^2 C_{g0}^2/h_0 \propto h_0^{-1}$ for small h_0 when h_0/h_1 and α_0 are fixed. It follows from figure 5 and (4.7) that

$$\theta_1 \lesseqgtr \theta_0 \quad \text{if} \quad h_1 \lesseqgtr h_0.$$

Both θ_0 and θ_1 increase for decreasing α_0. In general the directions of the short wave, the envelope and the radiated free waves are all different.

5. Zone of variable depth

Referring to (3.15), we decompose ξ into two parts:

$$\xi = \xi_L(X)\exp\left(2i\int_{X_0}^{X} K_x\,dX\right)+\xi_F(X), \tag{5.1}$$

where ξ_L has the same formal expression as (4.2) except that h and k refer to their local values and depend on X. The dimensionless equation for ξ_F is then obtained straightforwardly from (3.15):

$$\frac{d}{dX}\left(h\frac{d\xi_F}{dX}\right)+(4(\Omega^2-k_y^2 h)\,\xi_F = G(X), \tag{5.2a}$$

where

$$G(X) = \left\{\frac{2b^2}{1+b^2}\left[h\frac{d^2Z}{dX^2}+\frac{dh}{dX}\frac{dZ}{dX}+i\left(4hK_x\frac{dZ}{dX}+2Z\frac{d}{dX}(K_x h)\right)\right]\right.$$
$$\left.-\frac{ib}{2}(C_g)_0^2 k_0^2\cos\alpha_0\frac{d}{dX}\frac{k}{C_g}\right\}\exp\left(2i\int_{X_0}^{X}K_x\,dX\right), \tag{5.2b}$$

$$Z = \xi_0-\xi_L. \tag{5.2c}$$

Since $G \neq 0$ in $X_0 < X < X$, ξ_F is now *forced* in the zone of variable depth (while *free* outside). As boundary conditions, the value and the derivative of ξ_F must match those of $(\xi_F)_j$ at $X = X_j$, i.e.

$$\xi_F = (\xi_F)_j, \quad \frac{d\xi_F}{dX} = \frac{d(\xi_F)_j}{dX} \quad \text{at} \quad X = X_j, \tag{5.3a, b}$$

where $(\xi_F)_j, j = 0, 1$, are formally expressed by (4.6) or (4.8) with unknown amplitudes B_j. Except for the uninteresting case where the depth change is very small, the solution must be obtained numerically. An efficient approach is to recast the boundary-value problem for ξ_F and $(\xi_F)_j$ subject to (5.3a, b) as a variational principle with the following functional:

$$J(\xi_F, B_0, B_1) = \int_{X_0}^{X_1} \mathrm{d}X\,[-\tfrac{1}{2}h(\xi_F')^2 + 2h\lambda^2\xi_F^2 - F\xi_F] \\ + h_0[\tfrac{1}{2}(\xi_F)_0 - \xi_F]\,(\xi_F')_0 - h_1[\tfrac{1}{2}(\xi_F)_1 - \xi_F]\,(\xi_F')_1. \quad (5.4)$$

This variational principle is a convenient basis for applying the finite-element method to solve for ξ_F in $X_0 < X < X_1$ and B_0 and B_1 numerically. Derivation of (5.4) and other details are similar to Foda & Mei (1982) and are also given in Benmoussa (1983); they are omitted here. The computer program has been checked against a semi-analytical solution for a linear transition between h_0 and h_1. Using element size 0.02 and double precision (needed for evaluating the forcing term G which involves second derivatives), the two solutions differ by 0.1 %. The numerical results for ξ_F will be discussed for three cases.

We remark here that the main part of Molin's (1982) paper is concerned with the special case of normal incidence and moderately deep water ($1 \gg kh \gg 1/\epsilon$). In particular, the steady set-down was ignored; the resulting amplitude of ξ_F is much smaller than $O(kA^2)$. Molin also gave some calculated results for $kh = O(1)$, by simply using (2.2), (2.4) and (3.4) instead of their deep-water limits. Thus the third term in (2.8) is missing from his theory.

Case I: A plane slope connecting two unequal but constant depths

There are four parameters in this problem: h_0, h_1, L and α_0. The initial amplitude ratio is taken to be $b = 1$, as its effect is only of quantitative interest.

We first fix the topography. The normalized constant depths are $h = 0.5$ and 1, and the normalized length of the transition is $L = 1$. In physical terms $k_\infty h = 0.5, 1$ and $\epsilon k_\infty L = 1$; the bottom slope is $\frac{1}{2}\epsilon$, where ϵ is the small rate of envelope modulation. Let the incident wave approach from the shallower water, i.e. $h_0 = 0.5$ and $h_1 = 1$. Figure 6(*a*) gives the amplitude of ξ_F over the slope; the phase of ξ_F is less interesting and is not presented. Suffice it to say that the X-derivative of the phase of ξ_F, say S, corresponds to the wavenumber component of the free wave in the x-direction. If $S > 0$ (or < 0), the free wave propagates to the right (or to the left). From the computer output of the phase we have checked that the radiation condition is satisfied as imposed. The amplitude of ξ_F is greater on the transmission (deeper) side of $X = X_1$ than on the incidence side $X = X_0$. For $\alpha_0 = \frac{1}{4}\pi$ there is a critical depth $h_* = 0.6$ at $X = 0.22$ (marked by the dashed line); the free wave ξ_F is now radiated only on the shallow (incidence side) but exponentially decaying on the deeper (transmission) side. Figure 6(*b*) shows the results for incident waves advancing from deeper water for the same topography. Again for $\alpha_0 = 0$ and $\frac{1}{6}\pi$, free waves are radiated towards both left ($X \to -\infty$) and right ($X \to +\infty$); the radiation being stronger on the transmission side, in qualitative agreement with Molin's result for $kh \gg 1$ and $\alpha_0 = 0$. For $\alpha_0 = \frac{1}{4}\pi$, free waves are only radiated on the shallower (transmission) side.

We have studied the effect of greater depth by fixing $\alpha_0 = 0°$ and the bottom slope $\mathrm{d}h/\mathrm{d}X = 0.5$, i.e. $L = 1$, $h_1 - h_0 = 0.5$. The results are qualitatively similar to figures 6(*a, b*), but the radiated long wave decreases monotonically in amplitudes with increasing h_0; the result is not presented here.

Next the transition zone is lengthened to $L = 5$, but the depth difference is kept at 0.5; the bottom slope is therefore reduced to $\frac{1}{10}\epsilon$. For short waves advancing from $h_0 = 0.5$ to $h_1 = 1$, the results are shown in figure 7(*a*). Radiation occurs for both sides

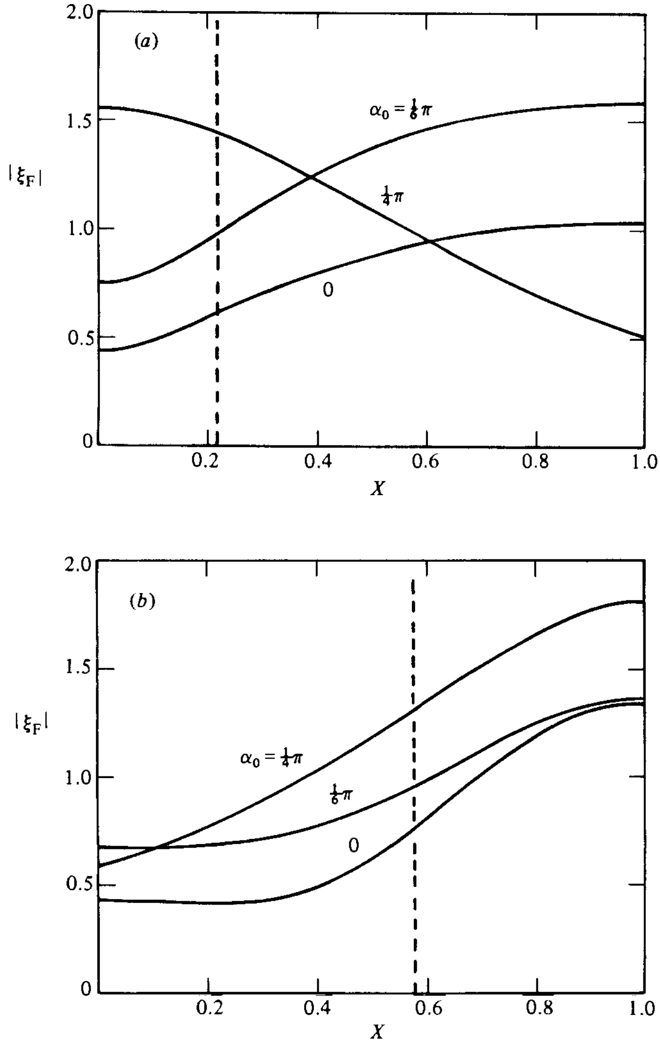

FIGURE 6. Amplitude of free long waves over a plane slope connecting two different depths. Dashed lines mark the locations of critical depth h_* for $\alpha_0 = \frac{1}{4}\pi$. Dimensionless length of slope $L = 1$. (*a*) $h_0 = 0.5$, $h_1 = 1.0$; (*b*) $h_0 = 1.0$, $h_1 = 0.5$.

of the transition but is stronger on the transmission (deeper) side. The maximum amplitude is of course reduced because of the milder slope. For $\alpha_0 = \frac{1}{4}\pi$ radiation is only toward the (shallow) incidence side, the critical depth occurs at $X \approx 1$. Within $X_0 < X < X_1$ the attenuation to the left is not exponential, because of the presence of forcing, but is exponential outside. If the short waves advance from the deeper ($h_0 = 1$) to the shallower ($h_1 = 0.5$) water, the amplitude of ξ_F varies in an oscillatory manner along the slope also (figure 7*b*). This oscillatory variation is due to interference and was also noted by Molin for normal incidence.

Finally we consider a whole range of transition length $0.5 < L < 5$ by keeping $h_1 - h_0 = \pm 0.5$, for normal incidence ($\alpha_0 = 0$) only. Radiation of ξ_F is stronger on the transmission side and decreased steadily with L whether the short waves advance from the shallower or from the deeper water, as shown in figure 8.

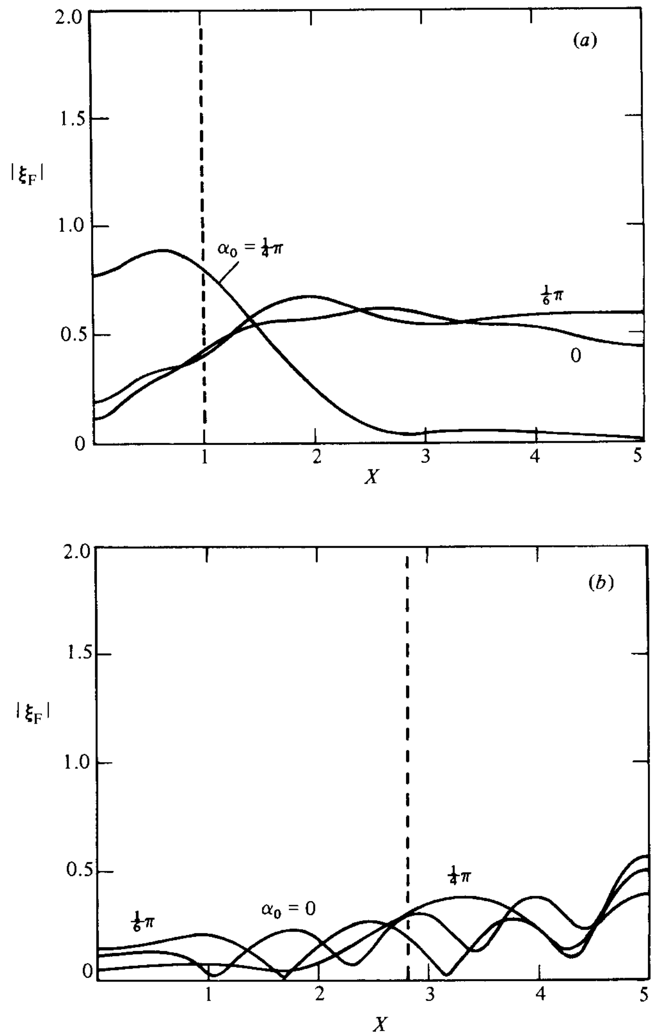

FIGURE 7. Same as figure 6 except $L = 5$. h_* is for $\alpha_0 = \frac{1}{4}\pi$. (a) $h_0 = 0.5$, $h_1 = 1.0$; (b) $h_0 = 1.0$, $h_1 = 0.5$.

For a large angle of incidence, say $\alpha_0 = \frac{1}{4}\pi$, radiation on the shallower side decreases with L. There is no radiation on the deeper side, because of the presence of the critical depth h_*. Numerical results are omitted.

Case II: Ridges. Case III: Canyons

Here we take $b = 1$ also and

$$\left.\begin{aligned} h &= h_0 + \frac{\Delta h}{2}\left(1 - \cos\frac{2X}{L}\right) \quad (0 < X < L), \\ &= h_0 \quad (X < 0 \quad \text{and} \quad X > L). \end{aligned}\right\} \tag{5.5}$$

Figure 9(a) shows the free wave for a ridge with $h_0 = 1.0$ and $\Delta h = -0.5$ and $L = X_1 - X_0 = 2$. For small angles of incidence $\alpha_0 = 0$ and $\frac{1}{6}\pi$, ξ_F is radiated to both

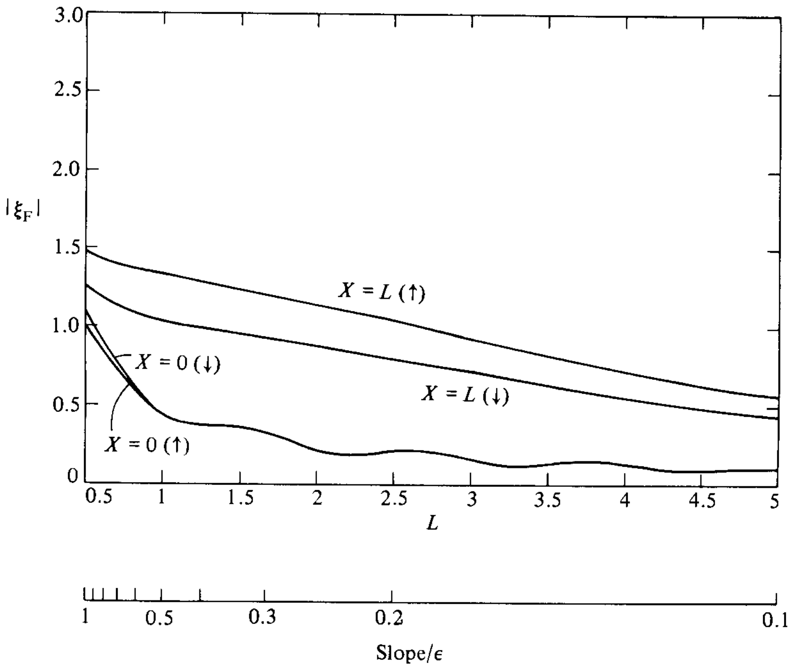

FIGURE 8. Amplitude of free long waves at the left and right edges of the slope as a function of slope length. Normal incidence. (↓) from $h_0 = 0.5$ to $h_1 = 1.0$; (↑) from $h = 1.0$ to $h = 0.5$.

$X \rightarrow +\infty$ and $-\infty$. The amplitude of ξ_F is not monotonic in X, but radiation is stronger on the transmission side. For a larger angle of incidence $\alpha_0 = \frac{1}{4}\pi$ two critical depths appear as marked by the dashed lines; ξ_F is generally larger between them and decays exponentially outside. Thus, while the short waves pass over the ridge, ξ_F is trapped on the ridge and propagates only along the ridge, which acts as a waveguide! Figure 9(*b*) shows the results for a wider ridge with $L = X_1 - X_0 = 10$ and the same $h_0 = 1.0$ and $\Delta h = -0.5$. For $\alpha_0 = 0$ and $\frac{1}{6}\pi$, $|\xi_F|$ generally increases in X; radiation is now much stronger on the transmission side. For $\alpha_0 = \frac{1}{4}\pi$ trapping between the two equal critical depths, i.e. the waveguide effect, is now more pronounced.

In figure 10(*a*) $|\xi_F|$ is plotted for a narrow canyon with $h_0 = 0.5$, $\Delta h = 0.5$ and $L = X_1 - X_0 = 2$. For small $\alpha_0 (= 0$ and $\frac{1}{6}\pi)$ $|\xi_F|$ is small and left-going at $X = 0$ and quite large and right-going at $X = L$; it changes rather little over the middle part of the canyon. For $\alpha_0 = \frac{1}{4}\pi$ the left-going wave at $X = 0$ is now much greater, while the right-going wave at $X = L$ is reduced. In the centre part of the canyon $|\xi_F|$ is suppressed. Thus the canyon acts as a barrier which causes greater backward radiation, and less forward radiation. Figure 10(*b*) is for a wider canyon with $L = 10h_0$ and Δh_0 being the same as before. Because of the milder slope $|\xi_F|$ there is an overall reduction of $|\xi_F|$. Especially noteworthy is the very low intensity between the two equal critical depths in the canyon for $\alpha_0 = \frac{1}{4}\pi$. Thus the barrier effect is further enhanced.

The effect of increasing canyon width L is not however monotonic, as is shown in figure 11 for normal incidence. In particular the radiation on the incidence side is generally much smaller and while the stronger radiation on the transmission side is oscillatory in L, as is qualitatively the case for the ridge.

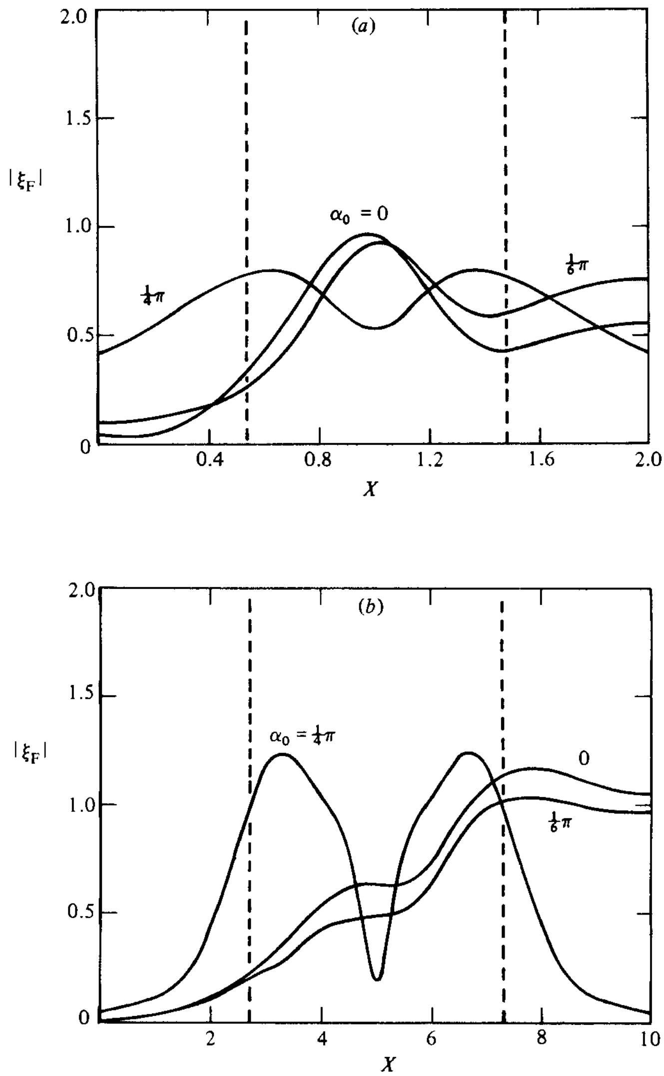

FIGURE 9. Amplitude of free long waves over a ridge $h_0 = 1.0$, $\Delta h = -0.5$. Dashed lines mark the locations of critical depth h_* for $\alpha_0 = \frac{1}{4}\pi$. (*a*) Width of canyon $L = 2$; (*b*) $L = 10$.

6. Concluding remarks

In this paper we have focused our attention on long waves caused by periodically modulated groups of short waves incident upon a variable bottom with straight and parallel contours. Because of nonlinearity, the radiation stresses induce steady set-down and long waves that are locked to the wave envelope. When there is a finite region of variable depth and the lengthscale of the region is comparable to the group length, further long waves are generated and radiated away as free long waves. These additional long waves have directions and propagation speeds different from those of the short waves, and of their envelope (hence also of those long waves which are locked to the envelope). There are also situations where these new long waves can be trapped on the shallow depth. We stress that, these free or trapped long waves

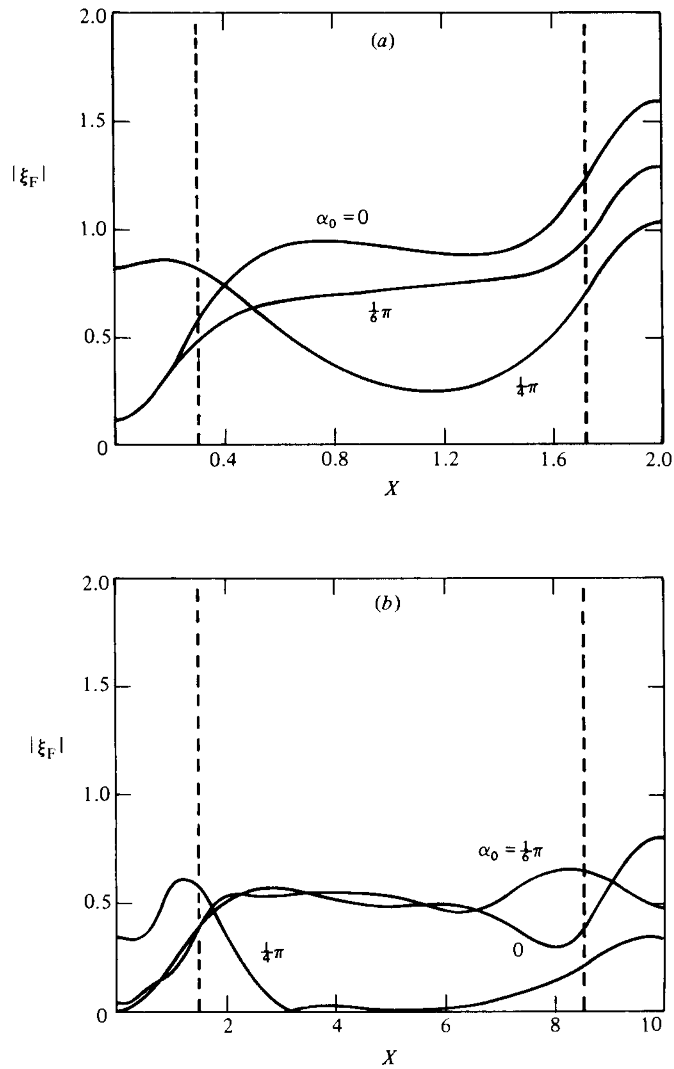

FIGURE 10. Amplitude of free long waves over a canyon, $h_0 = 0.5$, $\Delta h = -0.5$. Dashed lines mark the locations of critical depth h_* for $\alpha_0 = \frac{1}{3}\pi$. (*a*) Width of canyon $L = 2$; (*b*) $L = 10$.

differ from those in earlier theories of Longuet-Higgins (1967) where the forcing mechanism by incident long waves was strictly linear.

In this study the incident wave is characterized only by the angle of incidence, whose effect is of primary importance to the phenomenon at hand. Other parameters which can describe incident waves of increasing complexity will certainly be of practical interest. For example, we can take the incident waves to consist of two collinear trains of unequal amplitudes, i.e. $b \neq 1$ in (3.3). The computation is straightforward, but clearly the generation of free and locked long waves is not qualitatively altered. In practice it may also be desirable to include the effects of a small directional spread and/or randomness in the incident waves; nevertheless (2.9) is still a proper starting point. For transient envelopes such as a wave packet, the numerical method of characteristics can then be used.

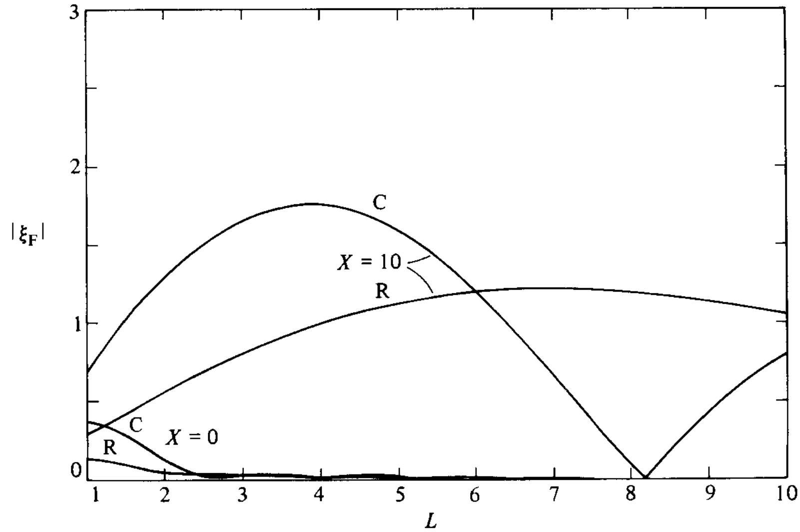

FIGURE 11. Amplitude of free long waves at the left and right edges of a canyon (C) $h_0 = 0.5$, $\Delta h = 0.5$ and a ridge (R) $h_0 = 1.0$, $\Delta h = -0.5$ as a function of width L. Normal incidence only.

Extension of the present study to two-dimensional submerged shoals should be worth while. Except for the neighbourhood of a caustic, the short-wave envelope may then be solved by the method of characteristics from (2.6); the free waves can also be effectively computed by the two-dimensional hybrid-element method of Chen & Mei (1974). Refinement near a caustic where diffraction takes place is desirable. On the other hand, a large-scale shear current also refracts short waves at the first order. Analogous generation of long waves at the second order is then expected, and extensions of (2.7) and (2.8) are a very convenient basis for treating these waves. Further studies on the resonance of small fishing harbours by long groups of short waves, in which diffraction (rather than refraction) of the modulated short waves is the primary feature, will also be very valuable to coastal engineering.

This research was initiated when CCM was a NTNF Senior Scientist at the Norwegian Institute of Technology, Trondheim. Supports by the Fluid Dynamics Program of Office of Naval Research and the Mechanical Engineering Program of National Science Foundation, are acknowledged by both authors with pleasure. Comments by the referees and Dr D. H. Peregrine have been most helpful.

REFERENCES

BENMOUSSA, C. 1983 Wave–current interaction over uneven topography. M.S. thesis, Department of Civil Engineering, Massachusetts Institute of Technology.

BOWEN, A. J. 1969 The generation of longshore currents on a plane beach. *J. Mar. Res.* **27**, 206–214.

BOWERS, E. C. 1977 Harbour resonance due to set-down beneath wave groups. *J. Fluid Mech.* **79**, 71–92.

BURNSIDE, W. 1915 On the modulation of a train of waves as it advances into shallow water. *Proc. Lond. Math. Soc.* **14**, 131–133.

CHEN, H. S. & MEI, C. C. 1974 Oscillations and wave forces in an offshore harbor in the open sea. *Proc. 10th Symp. Naval Hydrodyn.*, pp. 573–594.

Chu, V. H. & Mei, C. C. 1970 On slowly varying Stokes waves. *J. Fluid Mech.* **41**, 873.

Foda, M. A. & Mei, C. C. 1981 Nonlinear excitation of long trapped waves by a group of short swells. *J. Fluid Mech.* **111**, 319–345.

Hansen, N.-E. O. 1978 Long period waves in natural wave trains. *Prog. Rep.* no. 46, *Tech. Univ. Denmark, Inst. Hydrodyn. and Hydraul. Engng*, pp. 13–24.

Lighthill, M. J. 1952 On sound generated aerodynamically. I. *Proc. R. Soc. Lond.* A **211**, 564–587.

Longuet-Higgins, M. S. 1967 On the trapping of wave energy around islands. *J. Fluid Mech.* **29**, 781–821.

Longuet-Higgins, M. S. 1970*a* Longshore currents generated by obliquely incident sea waves. Part 1. *J. Geophy. Res.* **75**, 6778–6789.

Longuet-Higgins, M. S. 1970*b* Longshore currents generated by obliquely incident sea waves. Part 2. *J. Geophys. Res.* **75**, 6790–6801.

Longuet-Higgins, M. S. & Stewart, R. W. 1960 Changes in the form of short gravity waves on long waves and tidal current. *J. Fluid Mech.* **8**, 565–583.

Longuet-Higgins, M. S. & Stewart, R. W. 1961 The changes in amplitude of short gravity waves on steady non-uniform currents. *J. Fluid Mech.* **10**, 529–549.

Longuet-Higgins, M. S. & Stewart, R. W. 1962 Radiation stress and mass transport in gravity waves, with application to 'surf-beats'. *J. Fluid Mech.* **13**, 481–504.

Mei, C. C. 1982 *The Applied Dynamics of Ocean Surface Waves.* Wiley Interscience.

Molin, B. 1982 On the generation of long-period second order free waves due to changes in the bottom profile. *Rapp. IFP*: 30167, *Inst. Français du Petrole.* [Also published as *Ship Res. Inst. Rep.* 68, *Tokyo, Japan.*]

Sand, S. E. 1982 Long wave problems in laboratory models. *J. Waterways, Port, Coastal & Ocean Div. ASCE* **108**(WW4), 492–503.

Thornton, E. B. 1970 Variation of longshore current across the surface zone. In *Proc. 12th Coastal Engng. Conf.* pp. 291–308. ASCE.